Dynamic Responses of the Low-speed Maglev Vehicle on the Curved Guideway

Chunfa ZHAO*, Wanming ZHAI**, Kaiyun WANG**

*State Key Laboratory of Traction Power, Southwest Jiaotong Univ., Chengdu 610031, China
Dept. of Appl. Mech. and Eng., Southwest Jiaotong University, Chengdu 610031, China
Phone: +086-028-87600773, Email: cfzhao@126.com
**Train & Track Research Institute, Southwest Jiaotong University, Chengdu 610031, China
Phone/Fax: +086-028-87601843, Email: wmzhai@home.swjtu.edu.cn

Keywords: maglev, curve negotiation, transition curve, dynamics, numerical simulation

Abstract

Firstly, a dynamic curving model of the low-speed maglev vehicle is established. And then, dynamic curving behaviors of the maglev vehicle are simulated and analyzed. Finally, curve negotiation performances are evaluated. Results show the CFC-01 low-speed maglev vehicle can negotiate safely the 300m-radius curve with the 1º cant angle at the speed of 60km/h, and can also negotiate smoothly the 1100m-radius curve without superelevation even if at the speed of 90km/h. It is concluded that the maximum curve negotiation speed of the low-speed maglev vehicle is restricted by both the mechanical vehicle/guideway clearances and the ride comfort limits.

1 Introduction

The low-speed EMS maglev vehicle mainly runs in the city as the urban transit, which means that a plenty of small radius curve has to be built. Therefore, studies on dynamic curving behavior of the maglev vehicle are necessary to obtain better curve negotiation performances. Moreover, the work can provide some theoretical evidences and basic data to improving the bogie structure and the curved guideway configuration.

First, this paper introduces the 300m-radius curve configuration on Qingcheng Mountain Maglev Demonstration Line. At the same time, the 1100m-radius curve without superelevation is designed for the future application. Second, a 35 degrees-of-freedom (DOF) dynamic curving model of the low-speed maglev vehicle is developed. Third, dynamic curving behaviors of the CFC-01 maglev vehicle (developed by Southwest Jiaotong University) on the 300m radius and the 1100m radius curved guideway are calculated respectively. Finally, curve negotiation performances of the CFC-01 maglev vehicle are evaluated according to the allowed lateral displacement of the magnet module and the unbalanced centrifugal acceleration limit.

The purposes of the paper are: (1) to explore the simulation method of the dynamic curving behaviors of the low-speed maglev vehicle; (2) to evaluate the curve negotiation performances of the CFC-01 maglev vehicle on the 300m-radius and 1100m-radius curved guideway; (3) to achieve the

theoretical evidences and data of the reasonable curve arrangement and the structural optimization of the low-speed maglev vehicle, especially the bogie structure.

2 Curved Guideway Arrangement

Because the running speed of the low-speed maglev vehicle is less than 100km/h, no superelevation is set on the large-radiused curve, which lowers the construction and maintenance costs. But superelevation is necessary for the small-radiused curve, which aids the magnet to produce enough lateral force when the maglev vehicle negotiates the curve. Minimum horizontal radius is restricted by the mechanical clearances between the maglev vehicle and guideway and also, by ride comfort limits at higher speed.

The curved guideway is composed of the transition curve and the circle curve. The minimum length of the transition curve is mainly limited by the allowed superelevation gradient, which is determined by the mechanical decoupling tolerance. For instance, the test track [1] for HSST-03 vehicle on EXPO'86 set up a segment of 250m-radius curve and a segment of 1100m-radius curve, the cant angle of the former is 1.15º and the sine transition curve is selected after comparing the single module simulation results of three types of transition curve, clothoid, cosine and sine, for the latter no superelevation is arranged. In the design of Qingcheng Moutain Maglev Demonstration Line [2], the 50m-length clothoid transition segment and 1º cant angle is arranged for the 300m-radius curve, but there is no superelevation for the curves whose radius is more than 1000m. Based on the above-mentioned curved guideway, in the paper, the 300m-radius curve is taken as the first curve for the following simulation; the 1100m-radius curve is the second.

Fig.1 shows the horizontal and vertical configuration of the clothoid transition segment. In Fig.1, i is the gradient, l the distance, h the superelevation, l_0 the length of the transition segment, R_0 and h_0 is the radius and superelevation of the circle curve respectively. It is noted that the clothoid transition segment involves the break angle in the vertical plane as showed in Fig.1, which give a strong impact to the maglev vehicle in the start-point and the end-point of the transition segment. So the improved clothoid transition curve [3] in Fig.2 is adopted to depress the impact. Fig.2 indicates that a tangent circular arc replaces the break point, which smoothes the superelevation.

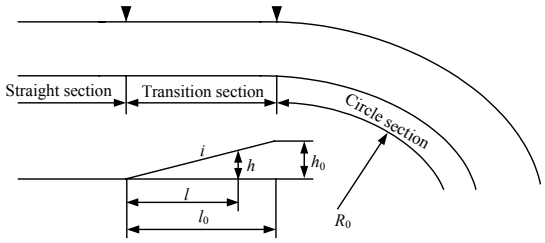

Fig.1 Clothoid transition curve

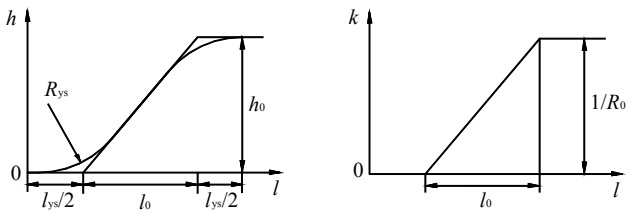

Fig.2 Smoothed clothoid transition curve

3 Dynamic Curving Model of the Low-speed Maglev Vehicle

3.1 Spatial model

The low-speed EMS maglev vehicle, such as HSST-100 [4], CFC-01 [2] and CMS-03 [5] (developed by National University of Defense Technology), are characterized by the module structure consisting of a LIM for propulsion and four magnets for levitation and guidance. The bogie consists of two modules and four pieces of anti-roll beam, and the bogie supports the car body through secondary air spring. Moreover, the lateral slide support and the tightwire guidance framework are used to enhance the curve negotiation performance of the vehicle. Fig.3 shows the bogie structure of the CFC-01 maglev vehicle.

Assuming that components of maglev vehicle are rigid bodies, a 35-DOF spatial model of maglev vehicle is established considering vertical, lateral, sway, pitch and roll motions, as showed in Fig4~6.

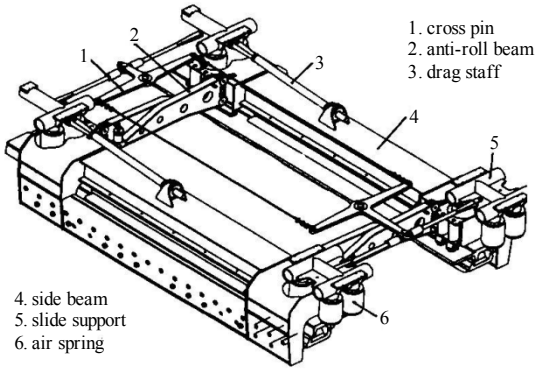

Fig.3 Bogie of CFC-01 maglev vehicle

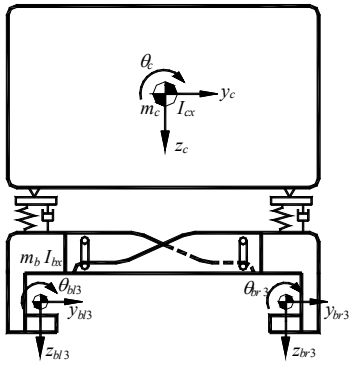

Fig.4 End view of the vehicle model

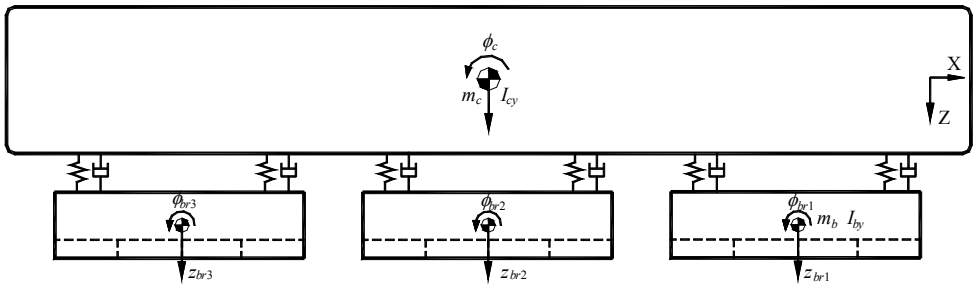

Fig.5 Elevation view of the maglev vehicle model

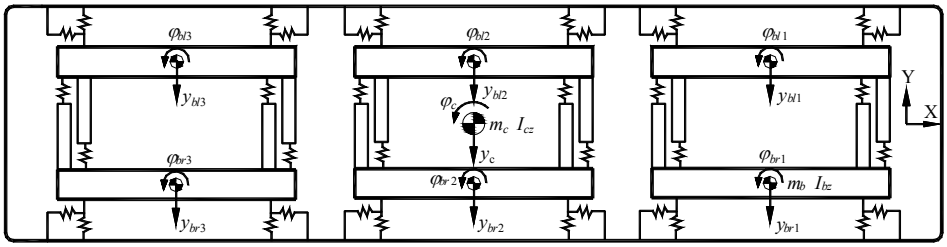

Fig.6 Plan view of the maglev vehicle model

3.2 Axis Systems

Fig.7 demonstrates the module following the curved guideway. To define completely the motions of the maglev vehicle, four moving axis systems are used, as shown in Fig.8. A guideway reference frame is used to describe the inertial acceleration of the components. The axis systems with subscripts *c*, *bl* and *br* correspond to the carbody, the left and the right modules respectively. The relationships of the component axis system and the guideway axis system are given as [6]

$$\begin{Bmatrix} \boldsymbol{i}_g \\ \boldsymbol{j}_g \\ \boldsymbol{k}_g \end{Bmatrix} = \begin{bmatrix} 1 & -\alpha & 0 \\ \alpha & 1 & -\beta \\ 0 & \beta & 1 \end{bmatrix} \begin{Bmatrix} \boldsymbol{i}_{c(b)} \\ \boldsymbol{j}_{c(b)} \\ \boldsymbol{k}_{c(b)} \end{Bmatrix} \tag{Eq.1}$$

where α and β are the angles of different longitudinal axes and radial axes respectively.

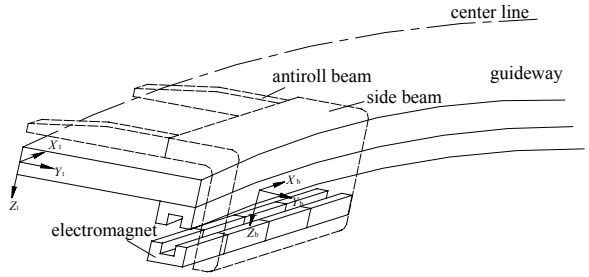

Fig.7 Module following the curve

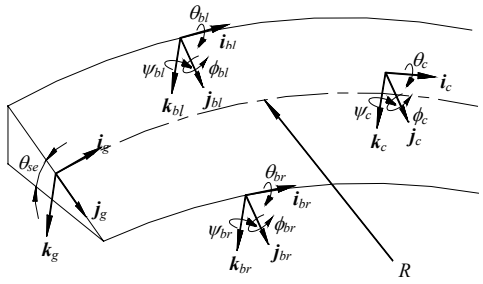

Fig.8 Definition of coordinate systems

4 Motion Equations and Solution

Assuming that the vehicle components are rigid bodies, motion equations of the maglev vehicle can be written as

$$\mathbf{M}\ddot{\mathbf{X}} + \mathbf{C}\dot{\mathbf{X}} + \mathbf{K}\mathbf{X} = \mathbf{F} \tag{Eq.2}$$

where **M, C** and **K** are the mass, damping and stiffness matrices of the maglev vehicle system respectively, $\mathbf{X}$ is the displacement vector, **F** the force vector containing the magnetic forces. Referring to literatures [7], the magnetic forces are expressed as

$$F_z = F_0 \left[1 + \frac{2\delta_z}{\pi W_m} + \frac{2\delta_y}{\pi W_m} \tan^{-1}\left(\frac{\delta_z}{\delta_y}\right) - \frac{|\delta_y|}{W_m} \right] \tag{Eq.3}$$

$$F_y = F_0 \left[\frac{2\delta_z}{\pi W_m} \tan^{-1}\left(\frac{\delta_y}{\delta_z}\right) \right] \tag{Eq.4}$$

where $F_0=\mu_0 A(NI/\delta_z)^2/4$, δ_z and δ_y is the vertical airgap and the lateral displacement of the magnet respectively, W_m and A is the width and area of magnetic pole, μ_0 the permeability of free space, I the current through the magnet windings, N the number of turns of the windings. The current control law is considered as follows [8]

$$\Delta I = k_{p1}\delta_z + k_{v1}\dot{\delta}_z + k_{a1}\ddot{\delta}_z \pm k_{v2}\dot{\delta}_y \quad \text{(Eq.5)}$$

where k_{p1}, k_{v1} and k_{a1} are the feedback gains corresponding to of the change, the velocity and the acceleration of the levitation airgap, k_{v2} the feedback gain of the lateral airgap velocity.

A new fast explicit time integration algorithm developed by Zhai [9] based on the implicit Newmark method is adopted to solve the motion equations. This two-step method avoids solving linear algebraic equations as long as the mass matrix appears diagonal, and computational speed is much faster than those of other popular methods when it is applied to large-scale system dynamic analysis.

5 Simulation Results

To evaluate curve negotiation performances of the low-speed maglev vehicle, two guidelines are suggested [10]: (1) the maximum lateral displacement of module should be less than ±15mm considering the nominal clearance, 20mm, between the inside face of the module truck and the guide rail. Otherwise, the mechanical collision is extremely possible; (2) the maximum unbalanced centrifugal acceleration should be less than 0.4m/s^2 and can not be more than 0.6m/s^2 for better ride comfort.

In the simulation, the 300m-radius and 1100m-radius curve are arranged as listed in Table 1.

Table 1 Configurations of the curved guideway

Radius (m)	300	1100
Cant angle (degree)	1	0
Transition curve length (m)	50	20
Circle curve length (m)	70	96
Smoothed length (m)	40	0

5.1 Dynamic Responses on the 300m-radius Curve

Dynamic curving behaviors of the CFC-01 maglev vehicle on the 300m radius curve at the speed of 30, 45, 60 and 75km/h are simulated respectively, and the maximum unbalanced centrifugal accelerations are 0.06, 0.35, 0.75, 1.27m/s^2 correspondingly. Fig.9 and Fig.10 show the lateral displacement of the car body and the left No.1 (L1) module relating to the guideway. Fig.9 indicates that the car body moves outside when the running speed is more than 45km/h, which implies that the secondary suspension will bring larger lateral forces. Fig.10 shows the maximum lateral displacement of the L1 module is 2.3, 5.3, 9.4 and 14.4mm respectively, which occurs at the turning point from transition curve to circle curve. And the corresponding mechanical clearance between the module beam and the guide rail is 17.7, 14.7, 10.6 and 5.6mm.

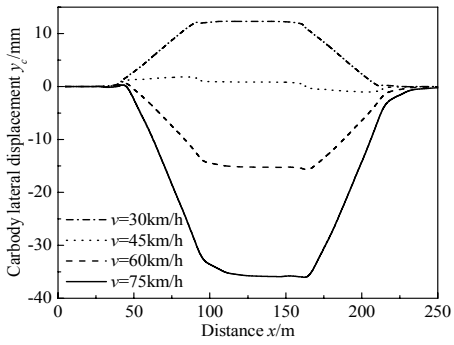

Fig.9 Lateral displacement of the carbody (R_0=300m)

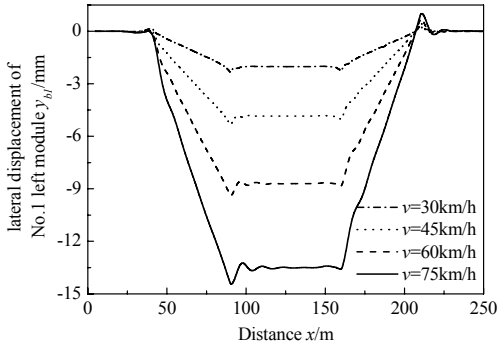

Fig.10 Lateral displacement of the L1 module (R_0=300m)

When the running speed is 60km/h, the levitation gaps and currents of four magnets on the L1 module are shown in Fig.11 and Fig.12. As is indicated in Fig.11, the levitation gaps exceed the nominal gap, and the maximum fluctuation is 1.35mm, which accords with the fact that the left magnetic force will decrease slightly because of the inner-tilting car body. Fig.12 shows that the maximum current appears when the vehicle enters or exits the transition segment, the maximum current of the four magnets is 39.4A (the nominal current is 28A).

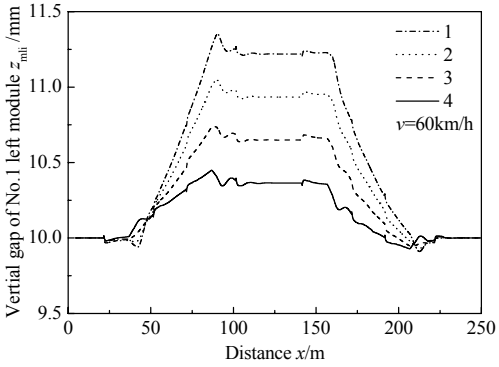

Fig.11 Vertical airgap of the magnet (R_0=300m, v=60km/h)

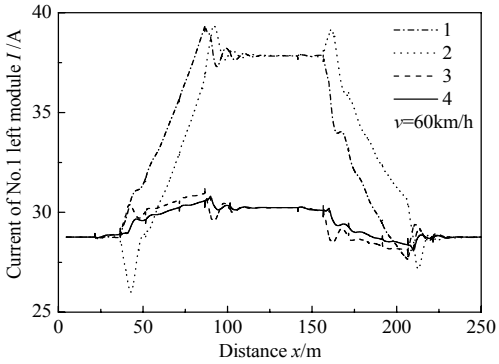

Fig.12 Current of the magnet windings (R_0=300m, v=60km/h)

5.2 Dynamics Responses on the 1100m-radius Curve

In this section, dynamic responses of the CFC-01 maglev vehicle at the speed of 45, 60, 75 and 90km/h are calculated respectively. As a result of no superelevation, the centripetal force of the maglev vehicle running on the curved guideway is provided by magnetic forces entirely. Simultaneously, the unbalanced lateral acceleration equals to the centripetal acceleration of the vehicle, it is 0.14, 0.25, 0.39, 0.57m/s^2 corresponding to the speed of 45, 60, 75, and 90km/h respectively. Fig.13 and Fig.14 show that the lateral displacement of the car body and the right No.1 (R1) module relating to the guideway. Fig. 13 reveals that the car body moves outside in all the four speed conditions, which implies that the secondary suspension provides the total centripetal force of the car body. And it is shown in Fig.14 that the maximum lateral displacement of the R1 module is 2.0, 3.4, 5.1 and 7.3mm respectively. So the minimum clearance between the R1 module and the guide rail is 12.7mm, it can be concluded that the mechanical collision can be avoided even if the CFC-01 vehicle runs on the 1100m radius curve at the speed of 90kmh.

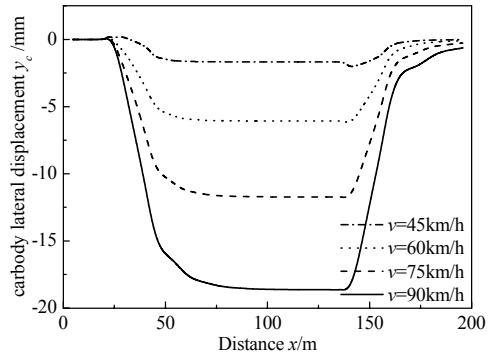

Fig.13 Lateral displacement of the carbody (R_0=1100m)

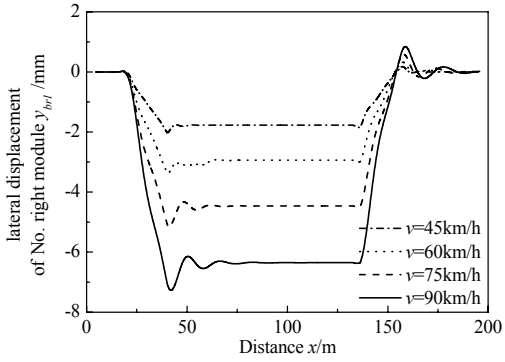

Fig.14 Lateral displacement of theR1 module (R_0=1100m)

Fig.15 and Fig.16 show the levitation gaps and currents of the four magnets on the R1 module when the running speed is 60km/h. As is shown in Fig.15, the levitation gap fluctuations are very small and the maximum is less than 0.4mm by reason that no tilting angles of the car body nearly equals to zero. Fig.16 indicates that the current fluctuations are less than ±4A.

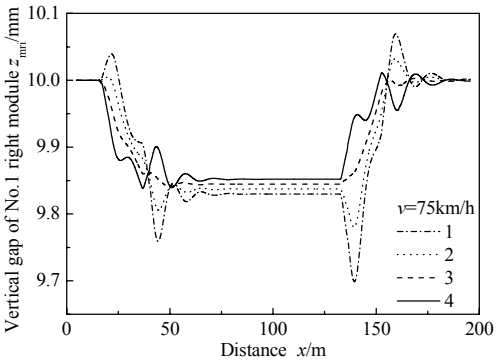

Fig.15 Vertical airgap of the magnet (R_0=1100m, v=75km/h)

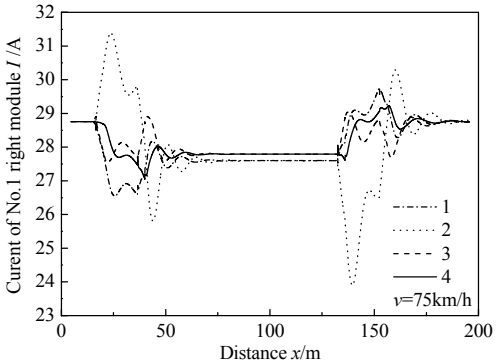

Fig.16 Current of the magnet windings (R_0=1100m, v=75km/h)

6 Conclusions

Based on the mature low-speed EMS maglev vehicle and maglev test track technology, the paper introduces the arrangements of the 300m-radius curve with 1º cant angle and the 1100m-radius curve without superelevation. And a 35-DOF dynamic curving model of the low-speed maglev vehicle is established. Dynamic curving behaviors of the CFC-01 maglev vehicle on the 300m-radius and 1100m-radius curved guideway are simulated by the numerical integration method. Simulation results and the assessments of curve negotiation performances of the low-speed maglev vehicle are as follows.

Firstly, when the CFC-01 maglev vehicle runs on the 300m-radius curve at the speed of 60km/h, the minimum clearance between the module and the guide rail is 10.1mm, which implies that the CFC-01 maglev vehicle can negotiates the curve smoothly, but the unbalanced centrifugal acceleration is $0.75/s^2$. In this case, the passengers can feel lateral thrust and less comfortable. If the running speed increases to 75km/h, the minimum clearance decreases to 3.73mm, so the mechanical collision between the module and the guide rail is very likely to occur. At the same time, the unbalanced

centrifugal acceleration is 1.27/s^2, which makes the passengers stand unsteadily and unable to walk. Hence, it is suggested that the maximum running speed of the CFC-01 maglev vehicle on the 300m-radius curve must be less than 60km/h.

Secondly, when the CFC-01 maglev vehicle negotiates the 1100m-radius and no superelevation curve, even if the running speed arrives at 90km/h, the maximum lateral displacement of the head module is only 7.4mm, so the mechanical collision is impossible to happen, but the unbalanced centrifugal acceleration is close to 0.6m/s^2, which makes the passengers feel little discomfort. Therefore, it can be concluded that superelevation is unnecessary for the curves whose radii are more than 1000m on the low-speed maglev line. But the maximum running speed should be restricted by the ride comfort limits.

7 Acknowledgments

The work described in this paper has been supported by National Natural Science Foundation of China (No.59975078), Applied Science Foundation of Sichuan Province (No.02GY029-040) and Science and Technology Development Foundation of Southwest Jiaotong University (No.2003A14). Their powerful supports are gratefully acknowledged.

References

1. Y Hosoda, M Kawashima, M Iwaya, Y Hikasa.: *Curvature running test results of HSST vehicle*. IEEE Transactions on Magnetics, 1987, MAG-23(5): 2344～2346
2. Anon.: *The Feasibility Report of Qingcheng Mountain Maglev Demonstration Line Project* (in Chinese). Chengdu: Southwest Jiaotong University, 1997
3. X.Z. Zhou. *A discussion on China's transition curve on high speed railway*. Journal of Southwest Jiaotong University, 1997, 31(1): 69-74
4. M. Fujino, M. Tanaka, S. Ishimoto. *Total test operation of HSST-100 and the project of East Hill-Side Line in Nagoya*. MAGLEV'2000. Rio de Janeiro, Brazil, 2000: 35-43
5. Anon.: *Technical Report of EMS Maglev Train key technology—Levitation and Guidance* (in Chinese). Changsha: National University of Defense Technology, 1996
6. V.K. Garg, R.V. Dukkipati. *Dynamics of Railway Vehicle Systems*. New York: Academic Press, 1984
7. E. Gottzein, K.H. Brock, E. Schneider, J. Pfefferl. *Control aspects of a tracked magnetic levitation high speed test vehicle*. Automatica, 1977, 13: 205～223
8. P.K. Sinha. *Electromagnetic Suspension Dynamics & Control*. London: Peter Peregrinus Ltd., 1987
9. W.M. Zhai. *Two simple fast integration methods for large-scale dynamic problems in engineering*. International Journal for Numerical Methods in Engineering, 1996, 39(24): 4199-4214
10. C.F. Zhao. *Maglev Vehicle System Dynamics* (in Chinese). Doctoral degree dissertation, Chengdu: Southwest Jiaotong University, 2002